Kinetics and Mechanism of the Oxidation of Methylene Violet by Bromate at Acidic pH and the Dual Role of Bromide Ion

S. B. Jonnalagadda* and M. N. Shezi

School of Chemistry, University of KwaZulu-Natal, Westville Campus, Chiltern Hills, P Bag X54001, Durban 4000, South Africa

Received: November 13, 2008; Revised Manuscript Received: March 19, 2009

Methylene violet (MV^+), a phenazine class of dye during oxidation by the bromate ion under acidic conditions, exhibited complex nonlinear behavior. The intricate kinetics of reaction of methylene violet [3-amino-7-(diethyleamino)-5-phenyl phenazium chloride, MV^+] with acidic bromate was investigated using the stopped flow technique. Under excess acid and bromate concentration conditions, MV^+ exhibited a very slow reaction initially but a very rapid reaction after an induction time. The reaction had first-order dependence on both H^+ and BrO_3^- ions. The overall stoichiometric reaction is

$$2MV^+ + 2BrO_3^- + H_2O \rightarrow 2MP + 2HON(CH_2CH_3)_2 + N_2O + 2H^+ + 2Br^-$$

where MP is the 3,7-dioxo-5-phenyl phenazine. The active roles of various bromo and oxybromo species in the mechanism are discussed. The rapid kinetics of the direct reaction of bromine with MV^+ is also reported. A 19-step mechanism, consistent with the experimental data and validated by simulations using Simkine-2, is proposed.

Introduction

Phenazines occupy a somewhat unique status in the field of organic chemistry. Quinoxaline alkaloids and other phenazine natural products exist. Phenazine dyes are widely used for cellulose and polyester blend fabrics (indanthrones and anthraquinone vat dyes) and for inks and printer toners (nigrosines).[1] Phenozine and phenoxazine dyes are extensively used as mordents to cotton and leather due to their stability, brilliant colors, and fastness to light. The bright colors associated with organic dyes are due to the presence of conjugated π bonds. In these dyes with extensive conjugate structure, the energy needed to effect electron promotion from the highest occupied to the lowest unoccupied molecular orbital falls within the UV−visible electromagnetic radiation range, hence exhibiting bright colors. The reactivity of these dyes under different conditions is pivotal in their applications as dyes under hostile conditions.[2] Mauveine, the first phenazine class of dye a purple compound discovered in 1856 by Hofmann's student Perkin and was manufactured on an industrial scale.[3]

Open systems such as stirred flow processes can easily generate and sustain bistability and oscillatory behavior. In the past three decades, numerous chemical reactions involving the bromate ion and demonstating temporal behavior such as the Belousov−Zhabotinsky (BZ) and uncatalyzed bromate oscillator (UBO) type reactions have been reported.[4−6] On the basis of the understanding of the mechanism of BZ reactions, numerous new oscillatory reactions have also been designed.[7]

Closed systems, during the oxidation of the heterocyclic dyes with acidic bromate, show intricate nonlinear behavior, unlike many aromatic compounds that exhibit temporal behavior. Earlier, we have reported the kinetics and reaction mechanisms of acidic bromate with phenothiazine and phenoxazine class of dyes.[8−11] In this communication we are reporting the studies on the kinetics and mechanism of the reaction of methylene violet with bromate in an acidic environment. Methylene violet (MV^+) also known as *N*,*N*-diethylsafranine is a phenazine class of water-soluble dye, with a sharp absorption peak in the visible region (λ_{max} = 557 nm, $\epsilon = 3.98 \pm 0.18 \times 10^4$ dm^3 mol^{-1} cm^{-1}). It shows no shift due to pH change and it is mildly toxic. Academic interest in the oxidation of methylene violet by the acidic bromate ion arises from the very slow initial reaction followed by a fast depletion, which is a typical characteristic of a nonlinear reaction. In this communication the kinetic results of oxidation of MV^+ both by acidic bromate and bromine are discussed and a probable mechanism validated by simulations is proposed.

Experimental Section

All chemicals were of Analar grade, and all the solutions were prepared in distilled water. Methylene violet chloride salt (Aldrich), potassium bromate (BDH), 98% sulfuric acid (BDH), and anhydrous sodium sulfate (Univar) were used as supplied.

Kinetic Measurements. All the kinetics were conducted at (25.0 ± 0.1) °C monitoring absorbance change of MV^+ (at 557 nm) using either Cary II- Varian UV−visible spectrophotometer or the double mixing microvolume stopped-flow (Hi-Tech Scientific SF-61DX2) spectrophotometer. Both the instruments were interfaced for data storage and have software to analyze the kinetic data. The MV^+/aqueous bromine kinetics were investigated using the stopped-flow apparatus. The bromide ion concentration, during the progress of reaction, was monitored using the bromide ion selective (Orion) and a double junction reference electrode. A HACH EC40 pH/ISE meter with digital data output was used to record the potential changes.

Results and Discussion

Product Analysis and Stoichiometry. For the oxidation product analysis, aqueous solutions of 50 mL of 0.01 M MV^+,

* To whom correspondence should be addressed. E-mail: jonnalagaddas@ukzn.ac.za.

10.1021/jp810015p CCC: $40.75
Published on Web 04/17/2009

TABLE 1: ^{1}H and ^{13}C Spectral Data of 3,7-Dioxo-5-phenyl-phenazine

position	δ_H (ppm), J (Hz)	δ_C (ppm)
1	7.16 (*d*, 8.5)	132.3
2	7.04 (*d*, 1.8)	121.0
3		216.4
4	5.61	116.8
6	5.84	117.1
7		216.8
8	7.08 (*d*, 8.5)	121.7
9	7.18 (*dd*, 8.5, 2.0)	132.8
1a		136.6
4a		137.0
5a		137.5
9a	3.12 (*d*, 7.3)	58.8
	aromatic region	
quaternary		135.5
o, *m*, and *p*	7.36−7.61 (*m*)	127.0, 131.2, 131.0

100 mL of 4.0 M sulfuric acid, and 200 mL of potassium bromate were mixed, and the resulting solution was allowed to stand for 72 h before further analysis. The reaction mixture was filtered and the filtrate neutralized with sodium bicarbonate producing a precipitate that was filtered and collected. The completion of the reaction was confirmed with thin-layer chromatography (TLC) plates against the starting material using 7:3 ratio of hexane and ethyl acetate as the eluent. The same solvent system was used to separate the products and using column packed with silica gel 60 (0.063−0.2, Merck). The presence of diethyl *N*-oxime $\{(C_2H_5)_2N\text{-}OH\}$ as one of the products was confirmed by TLC.

The major oxidation product was positively identified as 3,7-dioxo-5-phenyl-phenazine using mass spectrometry, infrared, and ^{1}H and ^{13}C NMR spectroscopy techniques. It was obtained as orange colored crystals with melting point of 112−115 °C. Its mass spectrum gave molecular ion peak at *m*/*z* 288 with other major fragment ions at *m*/*z* 211 (24), 105 (100), 87 (82), 72 (63), 55 (28). The IR spectrum gave absorption peaks at ν_{max} 1727 and 1633 cm^{-1}, which are characteristic of a ketone and a double bond, respectively.[12] The ^{1}H NMR showed a chemical shift value at δ 7.36−7.61 indicating the presence of a phenyl group which accounted for five methine protons as well as five methine and one quaternary carbons. In addition to these, seven other methine and five other quaternary carbons were also observed. Two of the quaternary carbons gave peaks at δ 216.4 and 216.8 in the ^{13}C NMR spectrum indicating the presence of two carbonyl groups. No signals were observed for methylene and methyl carbons. The methine protons resonated at δ 7.16 (*d*, 8.5 Hz), 7.04 (*d*, 8.5 Hz), 5.84, 5.61, 7.08 (*d*, 8.5 Hz), 7.18 (*dd*, 8.5, 2.0 Hz), and 3.12 (*d*, 7.3 Hz), and their respective positions are given in Table 1. The oxidation of substituted amino groups of substituted heterocyclic compounds (phenoxizine and phenozine dyes) to carbonyl groups under strong oxidizing conditions have been reported in the literature.[13,14] Although not confirmed in the present study, the formation of HNO and its final conversion to N_2O during the oxidation of hydroxyamines has been previously reported.[15] In addition, by using 1:20 and 1:50 molar ratios of $[MV^+]_0$:$[BrO_3^-]_0$ and an excess acid concentration, the stoichiometric ratio was determined in triplicate runs. The residual bromate concentration was established iodometrically by titrating with standard thiosulphate solution.[16,17] Under excess acid and bromate conditions, methylene violet reacted with bromate in a 1:1 stoichiometric ratio within ± 10% accuracy

$$2MV^+ + 2BrO_3^- + H_2O \rightarrow 2MP + 2HON(CH_2CH_3)_2 + N_2O + 2H^+ + 2Br^-$$

where MP is the 3,7-dioxo-5-phenyl phenazine.

On the basis of the chromatographic, spectrometric, and NMR analysis data, the major oxidation product of the reaction between MV^+ and bromine was also confirmed to be 3,7-dioxo-5-phenyl phenazine. The bromide ion was further oxidized to bromine in the presence of excess bromate as confirmed in this study.

Reaction Kinetics. All the reactions were studied at (25 ± 0.1) °C with excess initial concentrations of acid and oxidant and low $[MV^+]$. Figure 1a illustrates the repetitive spectra of the MV^+/acidic bromate reaction mixture between 300 and 700 nm and scanned at 20 s intervals (scan speed 50 nm s^{-1}) with initial reactant concentrations of $[H^+]_0$ 0.20 M, $[BrO_3^-]_0$ 0.01 M, and $[MV^+]_0$ 3.0×10^{-5} M. A perusal of Figure 1a shows that in the first few cycles, negligible changes occurred in the spectra and in subsequent scans the reaction rate increased and the substrate depleted quickly. The changes in the repetitive spectra as function of time indicate the formation of intermediates, having similarity with the substrate to much extent. The perusal of the visible spectrum of the main product, dioxo-5-phenyl phenazine (Figure 1b), shows a very strong absorption and with a slight shift in the spectrum toward longer wavelength in the <320 nm region and a broad/weak peak in the 500−600-nm region. A small absorption coefficient of (60 ± 5) dm^3 mol^{-1} cm^{-1} at about 540 nm confirmed the intactness of the aromatic structure but with a broken conjugate structure. The reaction progress for various reactions at varying initial concentrations of bromate was monitored at 557 nm in duplicate runs.

Figure 2 illustrates the absorbance vs time profiles of typical methylene violet consumption curves as function of bromate variation at constant ionic strength (I = 0.32 mol kg^{-1}). Unlike many bromate reactions with aromatic substrates, which display significant change in their concentration in the initial stages, the initial depletion of MV^+ was very slow, and after an induction time a transition occurred to fast depletion. For each kinetic run, the initial rate (r_i) (absorbance vs time ≈ 20−60 s) value was determined. The values from the duplicate runs had less than 5% deviation showing good reproducibility. The induction time (I_t) for the transition to rapid kinetics was estimated from the intersection of the tangents drawn to the sloping curves. The mean values of r_i and I_t from the duplicate runs for the bromate variation are summarized in Table 2. The plot of r_i vs $[BrO_3^-]_0$ plot was linear ($y = 7 \times 10^{-10}x - 2 \times 10^{-13}$; $R^2 = 0.998$) suggesting that the initial reaction rate has a first-order dependence on the initial bromate concentration, $[\text{bromate}]_0$. Similarly, the linearity of the $(1/I_t)$ vs $[BrO_3^-]_0$ plot ($y = 0.7585x - 0.00004$; $R^2 = 0.998$) confirms that the reaction that the transition to rapid kinetics had first-order dependence on the initial bromate concentration. The small values of negative *y* intercepts indicate that *x* intercepts were positive and suggest that certain critical minimum $[\text{bromate}]_0$ were needed for transition of the reaction to fast phase.

Dependence of Reaction Rate on Acid. The effect of $[H^+]_0$ on the reaction was studied at constant ionic strength (I = 0.91 mol kg^{-1}). The profiles of MV^+ concentration vs time curves at varied initial concentrations of acid are illustrated in Figure 3. Further, for each curve the kinetic data was analyzed for the initial rates and induction times and the analyzed data is summarized in Table 3. Both the r_i vs $[H^+]_0$ ($y = 3 \times 10^{-11}x - 8 \times 10^{-13}$, $R^2 = 0.997$) and the reciprocal I_t vs $[H^+]_0$ ($y = 0.03x - 0.0015$, $R^2 = 0.992$) plots were straight lines suggesting

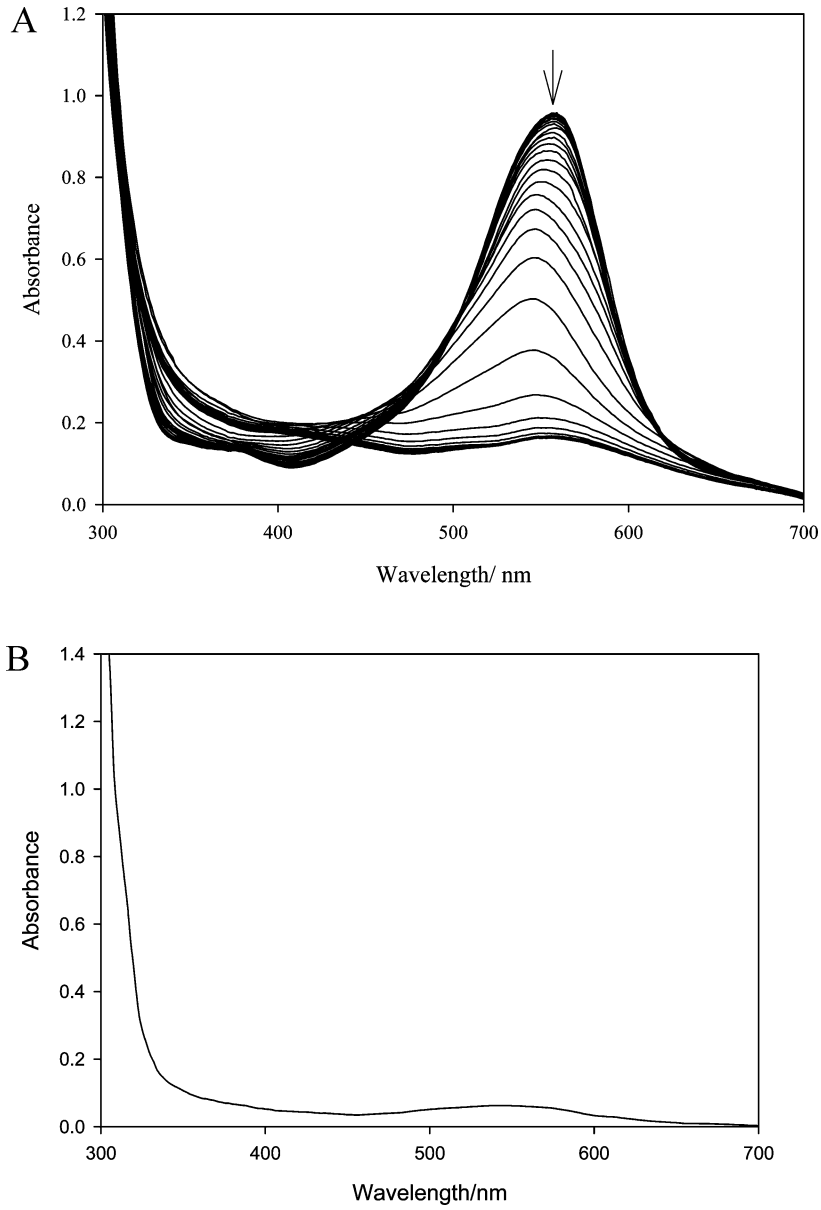

Figure 1. (a) Repetitive spectra: MV−acidic bromate reaction. $[MV^+]_0$ 3.0×10^{-5} M, $[H^+]_0$ 0.2 M, and $[BrO_3^-]_0$ 0.01 M. Scan rate 20 s per cycle. (b) Visible spectra of main product, 3,7-dioxo-5-phenyl phenazine (MP), in 5% alcohol. [MP] = 1×10^{-3} M.

TABLE 2: Effect of [bromate]$_0$ on the Kinetic Curves ($[MV^+]_0 = 3.0 \times 10^{-5}$ M; $[H^+]_0 = 0.20$ M, $\mu = 0.32$ mol kg^{-1})

$[BrO_3^-]_0/10^{-2}$ M	induction time[a], I_t/s	reciprocal I_t, $(1/I_t)/10^{-2}$ s^{-1}	initial rate[b], $r_i/10^{-11}$ M s^{-1}	rate constant[a] $k/10^{-4}$ M^{-2} s^{-1}	reference figure
0.35	330	0. 303	0.210	1.00	*2*a
0.55	225	0.444	0.321	0.97	*2*b
0.80	152	0. 658	0.512	1.07	*2*c
1.05	120	0.833	0.703	1.12	*2*d
1.40	88	1.136	0.912	1.09	*2*e
2.00	65	1.539	1.30	1.08	*2*f
		$k = (1.04 \pm 0.06) \times 10^{-4}$ M^{-2} s^{-1}			

[a] Mean of duplicate runs with <5% deviation. [b] Initial rate, $r_i = (\Delta Abs)/(\Delta Time\ x\xi)$, where ε is the absorption coefficient for MV^+ at 557 nm and rate constant, $k = (r_i)/([H^+][BrO_3^-][MV^+])$.

that the rates of the initial reaction and the rates of the rapid steps have first-order dependence on H^+ concentration. Further, the negative y-intercepts and resulting positive x intercepts, 0.025 M for the r_i vs $[H^+]_0$ plot and 0.05 M for the I_t^{-1} vs $[H^+]_0$ plot suggest that for a given $[BrO_3^-]_0$, a threshold minimum of $[H^+]_0$ is required for the reaction to occur and for the reaction's transition to rapid phase. Such a positive x intercept is obvious as the bromate ion is known to be passive at pH > 4 with no reactivity.[16]

Effect of Added Bromide on the Reaction. The role of Br^- ion as the controlled intermediate in the BZ type reactions is well documented.[4,5] The effect of the bromide ion on the kinetics of MV^+/bromate reaction was investigated by adding varying amounts bromide to the reactants under otherwise identical conditions. Figure 4 shows the profiles of the absorbance vs time plots. Curve a in Figure 4 represents the absorbance kinetic profile of MV^+ without extra added bromide. The increasing amounts of initially added bromide ($1.1-2.0 \times 10^{-6}$ M)

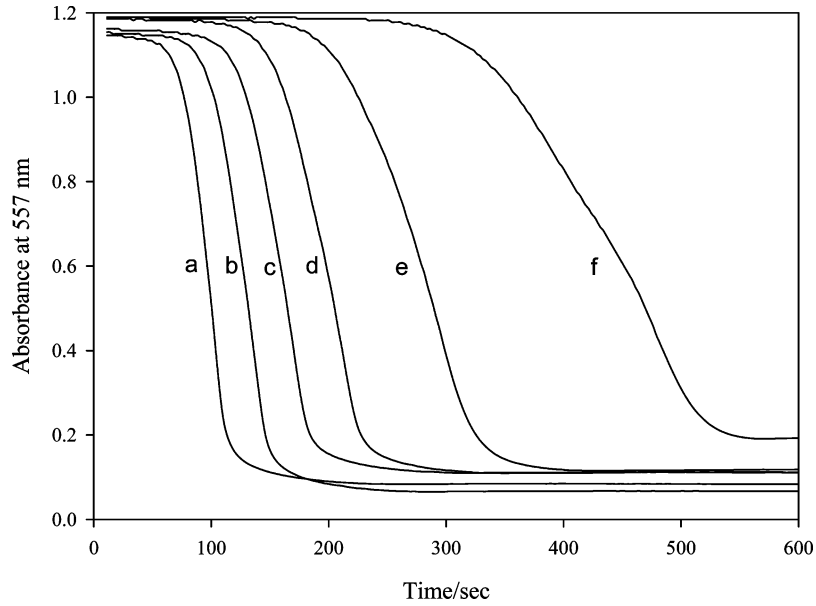

Figure 2. Typical nonlinear curves showing depletion of MV^+ at 557 nm with different initial [bromate]$_0$. $[MV^+]_0 = 3.0 \times 10^{-5}$ M, $[H^+]_0 = 0.2$ M, $[BrO_3^-]_0$/M = (a) 0.020, (b) 0.0125, (c) 0.009, (d) 0.007, (e) 0.0045, (f) 0.003.

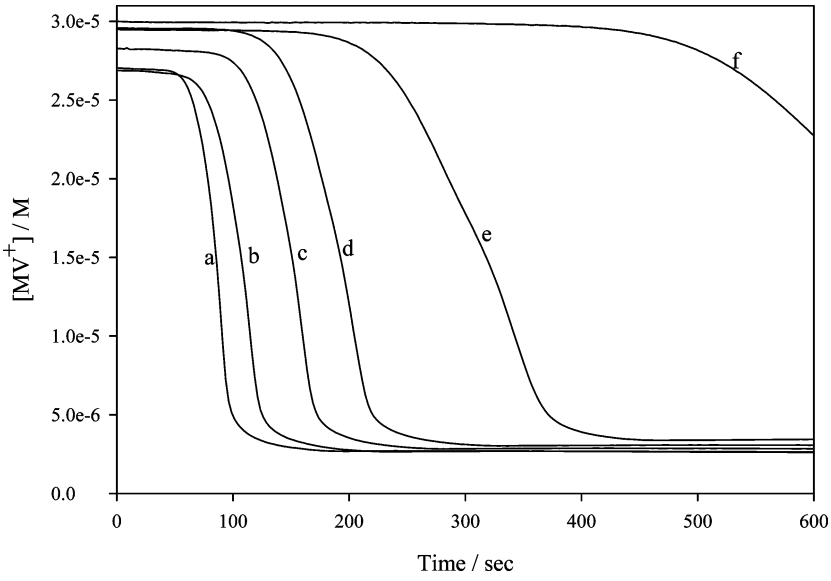

Figure 3. Effect of acid on the kinetic profiles of MV^+ depletion curves $[MV^+]_0 = 3.0 \times 10^{-5}$ M, $[BrO_3^-] = 0.01$ M, $[H^+]_0$/M = (a) 0.10, (b) 0.20, (c) 0.30, (d) 0.40, (e) 0.50, (f) 0.60.

marginally increased the initial oxidation rate, but interestingly it delayed the transition to the rapid phase, i.e., the induction times were increased (parts b−e of Figure 4). The further increase in $[Br^-]_0$ enhanced significantly the initial depletion rate of MV^+. Further, the MV^+ depletion curves lost their characteristic transition shape to one of the rapid phase kinetics (parts f−g of 4), resulting in an exponential decay of the dye. Such 2-fold role of the bromide ion as an inhibitor and autocatalyst under low and high concentration conditions, respectively, was observed for the reactions of methyl orange with bromine[18] and of indigo carmine with acidic bromate,[19] but no explanation for such behavior was reported. In the past, we reported on the mechanism and dual role of bromide during the oxidation of a phenazine class of dye, safranine-o, by acidic bromate.[14]

Bearing in mind that methylene violet is a chloride salt is used in the current study, the role of chloride ion on the reaction process cannot be ignored. The chloride ion is known to interact with the oxybromo species. It is well documented by the studies of Jacob et al.[20] demonstrating Cl^- role in BZ reactions through its reactions with $HOBr_2$, i.e.

$$Cl^- + HBrO_2 + H^+ \rightarrow HOBr + HOCl$$

and

$$HOCl + BrO_3^- + H^+ \rightarrow HBrO_2 + HClO_2$$

While the former reaction is thermodynamically favored ($E^\circ = 0.25$ V), the latter ($E^\circ = -0.40$ V) still can occur in presence of a high concentration of H^+ and bromate ions. HOCl could oxidize the organic species regenerating Cl^- or $HClO_2$ is could get further oxidized to ClO_3^- to be eliminated from the reaction chain.[20] The net reaction is represented by

TABLE 3: Effect of $[H^+]_0$ on the Kinetic Curves ($[MV^+]_0 = 3.0 \times 10^{-5}$ M; $[BrO_3^-]_0 = 0.010$ M and Ionic Strength, $\mu = 0.91$ mol kg^{-1})

$[H^+]_0$/M	induction time, I_t/s	reciprocal I_t, $(1/I_t)/10^{-2}$ s^{-1}	initial rate[a], $r_i/10^{-11}$ M s^{-1}	rate constant[b], $k/10^{-4}$ M^{-2} s^{-1}	reference figure
0.1	500	0.200	0.295	0.98	*3*a
0.2	223	0.448	0.608	1.01	*3*b
0.3	140	0.714	0.916	1.02	*3*c
0.4	100	1.00	1.24	1.03	*3*d
0.5	76	1.32	1.63	1.09	*3*e
0.6	58	1.72	2.01	1.12	*3*f
		$k = (1.04 \pm 0.05) \times 10^{-4}$ M^{-2} s^{-1}			

[a] Initial rate, $r_i = (\Delta Abs)/(\Delta Time\ x\xi)$ where ε is the absorption coefficient for MV^+ at 557 nm and rate constant, $k = (r_i)/([H^+][BrO_3^-][MV^+])$. [b] Mean of duplicate runs with less than 5% deviation (using the 10−60 s data for the abs vs time plots with R^2 varied between 0.95 to 0.98).

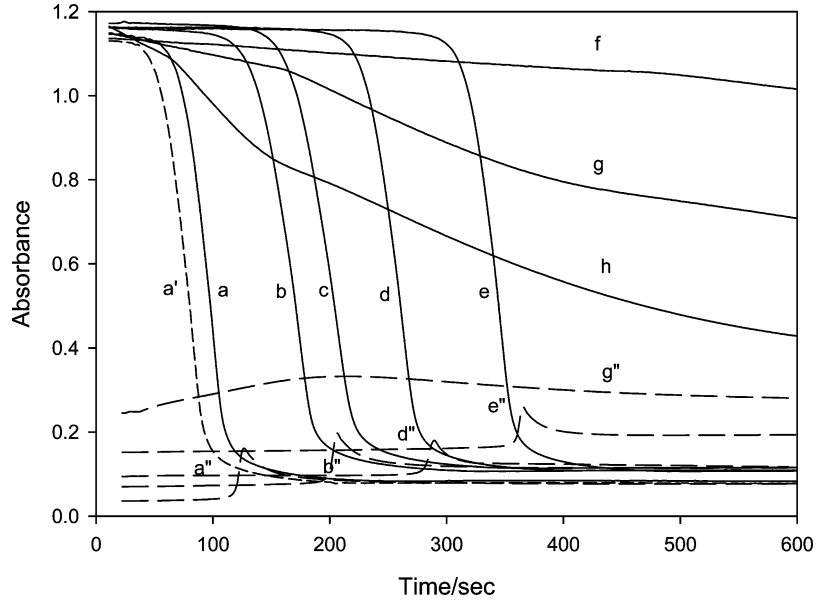

Figure 4. Effect of initial bromide on the kinetic profiles of MV^+ depletion and Br_2 formation. $[MV^+]_0 = 3.0 \times 10^{-5}$ M, $[H^+]_0 = 0.20$ M, $[BrO_3^-]_0 = 0.02$ M, and $[Br^-]_0$/M. Curve a and a″, nil; b and b″, 1.1×10^{-6}; c, 1.4×10^{-6}; d and d″, 1.7×10^{-6}; e and e″, 2.0×10^{-6}; f, 1.0×10^{-5}; g and g″, 2.0×10^{-5}; h, 1.0×10^{-4}. Curve a′, control curve with addition of 1.5×10^{-5} M Ag_2SO_4 to prior to experiment to remove the chloride in the solution.

$$2Cl^- + 2\ BrO_3^- + 3H^+ \rightarrow 3\ HOBr + 2\ ClO_3^-$$

Further in BZ type oscillations, Cl^- is known to interfere with the redox reactions of Ce(III)/Ce(IV) system, which is not applicable to the present study.[20]

During our earlier studies on the oxidation of Nile blue, a phenoxazine dye with acidic bromate, the kinetics of the reactions using both the chloride and sulfate salts of the dye under varied conditions were compared. The reactions with sulfate salts were found to have slightly shorter induction times than with chloride salts, but both salts exhibited the characteristic induction times followed by fast depletion of the substrates.[11] As a chloride salt of methylene violet is used in the current study, to establish its role, in a control experiment, a small amount of silver sulfate (2.5×10^{-5} M) was added to the MV^+ solution, and the solution was filtered after awhile and was used in the oxidation experiments. Curve a″ in Figure 4 was such control curve, which had about 10−12 min shorter induction time compared to the normal curve under otherwise identical conditions (curve a″ in Figure 4). Hence, in view of the small effect of chloride on the reaction trend, no further experiments were carried out to precipitate chloride ion. The observed marginal effect could also be due partial dissociation of the MV^+Cl^- salt.

Reaction of Bromine with MV$^+$. To establish the role of bromine in the reaction mechanism, the fast kinetics of the reaction between MV^+ and aqueous bromine were studied by using the stopped flow apparatus. The reaction was studied under using excess aqueous bromine conditions with low $[MV^+]_0$, and monitoring the depletion of MV^+ at 557 nm (Figure 5). Although the data was also fitting well for integrated rate expression for two competitive first-order reactions, only small coefficients were obtained for the second rate constant with no distinct trend. The ln abs versus time plots were straight lines confirming that reaction followed pseudo-first-order kinetics with respect to MV^+. With the increase in $[Br_2]_0$, the k'_{Br_2} values increased proportionately. Table 4 summarizes the results obtained with different $[Br_2]_0$. From the experiments, the second-order rate constant for the reaction between MV^+ and bromine is taken as 1.15×10^2 M^{-1} s^{-1}. The high rate coefficient for Br_2 confirms the role of bromine as the reactive intermediate in the overall reaction. Thus, under acidic conditions, HOBr is consumed either by conversion to bromine or through direct oxidation with the substrate and with the other reaction intermediates.

Reaction Mechanism. In BZ-type oscillatory chemical systems, the bromide ion acts as control intermediate and switches between high and low concentration conditions. The drop from high $[Br^-]$ to low occurs through the reaction of bromide with $HBrO_2$ and BrO_3^-. The regeneration of Br^- depends upon the nature of the organic species and its reaction

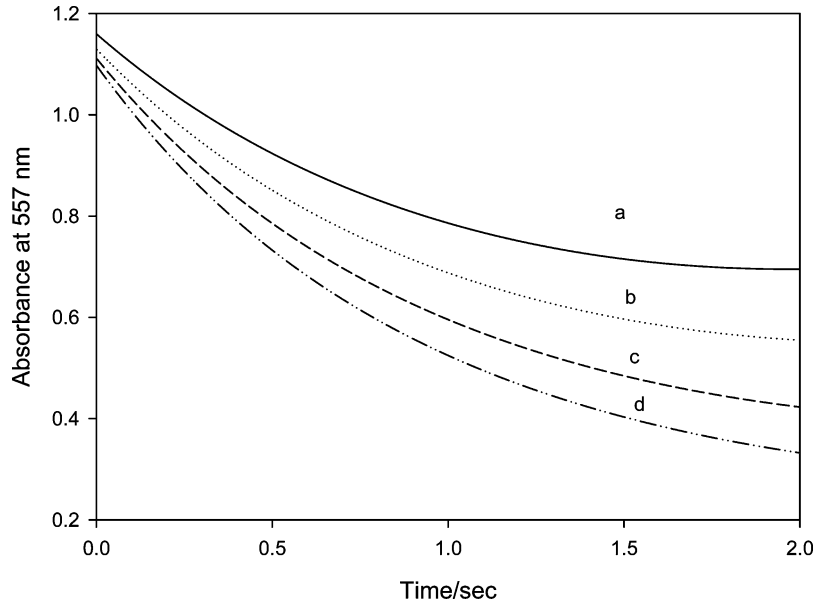

Figure 5. Kinetics of reaction between bromine and MV^+. $[MV^+]_0 = 3.0 \times 10^{-5}$ M and $[Br_2]_0/10^{-3}$ = (a) 2.44 M, (b) 3.24 M, (c) 4.06 M, (d) 4.88 M.

TABLE 4: MV^+ Reaction with Aqueous Bromine ($[MV^+] = 3.0 \times 10^{-5}$ M)

$[Br_2]_0/10^{-3}$ M	$k'_{Br_2}{}^a/s^{-1}$	$k_{Br_2}/10^2 M^{-1} s^{-1}$
2.44	0.256	1.05
3.24	0.357	1.10
4.06	0.488	1.20
4.88	0.599	1.23

$k_{Br_2} = (1.15 \pm 0.08) \times 10^2 M^{-1} s^{-1}$

[a] Mean of five runs with less than 5% deviation and $k_{Br_2} = k'_{Br_2}/[Br_2]_0$.

rate with the various oxybromo and bromo intermediates in the system. The crucial equations representing the chemistry of bromo and oxybromo intermediates in the reaction of bromate under acidic conditions shown below[4,5,21]

$$2H^+ + Br^- + BrO_2^- \rightleftharpoons HOBr + HBrO_2 \quad (R1)$$

$$H^+ + Br^- + HBrO_2 \rightleftharpoons 2HOBr \quad (R2)$$

$$H^+ + Br^- + HOBr \rightleftharpoons Br_2 + H_2O \quad (R3)$$

$$HBrO_2 + H^+ \rightleftharpoons H_2BrO_2^- \quad (R4)$$

$$HBrO_2 + H_2BrO_2^+ \rightleftharpoons 2H^+ + HOBr + BrO_3^- \quad (R5)$$

$$H^+ + BrO_3^- + HBrO_2 \rightleftharpoons 2Br_2O_4 + H_2O \quad (R6)$$

$$BR_2O_4 \rightleftharpoons 2BRO_2^* \quad (R7)$$

In the MV^+/acidic bromate system (in the absence of initially added bromide), the induction time reflects the time required for the accumulation of $HBrO_2$ and for the removal of inhibiting species, including bromide and the trace impurities with bromate. The rate-limiting step in such a system is the direct reaction between MV^+ and BrO_3^- in presence of acid, which is followed by the formation of the $[BrO_2^{*}]$ radical.[14,21]

The reactions of organic intermediates with BrO_3^-, $HBrO_2$, and HOBr are retarded by high [bromide] through its competitive reaction with the oxybromo species. High [bromide] inhibits the autocatalysis step (R6) by way of R2, thus depleting the $[HBrO_2]$. Hence it may be seen that the presence of bromide consumes $HBrO_2$ and thus prolongs the induction period for the rapid depletion of MV^+. The fast depletion step is the result of the rapid reaction of MV^+ with Br_2 and HOBr. The increased concentration of $HBrO_2$ enhances its disproportion rate. At high $[HBrO_2]$, with the bromide concentration at a critical level, bromide acts as an auto catalyst (R3), resulting in an increase in [HOBr]. Both Br_2 and HOBr could react rapidly with MV^+ and other organic species leading to the fast depletion of the organic substrate. Relative levels of HOBr and Br_2 are controlled by the concentrations of H^+ and Br^- ions (R4). The increased levels of $HBrO_2$ accelerate the formation of the reactive intermediate, $[BrO_2^*]$, through reactions R6 and R7. In addition, $HBrO_2$ also directly reacts with the organic intermediates.[4,14]

In MV^+/acidic bromate reactions, in the absence of added bromide, the initial rate limiting, slow reaction is attributable to interaction between the MV^+, H^+ and BrO_3^- ions (R8). The fast depletion step is the result of the rapid reaction of MV^+ with the reaction intermediates, bromine, and hypobromous acid. The oxidation of MV^+ occurs via the initial attack of bromate on the primary amino group resulting in −NH-OH as a transient intermediate leading to the formation of the carbonyl group. The positive charge on the N atom in the heterocyclic ring is known to facilitate the de-ethylation and hydrolysis, resulting in weakening of the conjugated structure leading to color loss by the oxidation product.[13,22] Furthermore, as the resulting product is nonionic, its solubility in water will also be less. On the basis of the kinetic and product data, the following simplified steps may be proposed of the oxidation of MV^+ (3-amino-7-(diethyleamino)-5-phenyl phenazium ion) to MP (3,7-dioxo-5-phenyl phenazine)

$$MV^+ + BrO_3^- + H^+ \rightarrow MA + HBrO_2 + NH_2OH + H^+ \quad (R8)$$

$$MV^+ + BrO_2^* \rightarrow MVR^+ + HBrO_2 \quad (R9)$$

$$MVR^+ + BrO_2^* \rightarrow MA + HBrO_2 + NH_2OH + H^+ \quad (R10)$$

$$MV^+ + HOBr \rightarrow MA + Br^- + 2H^+ + NH_2OH \quad (R11)$$

$$MV^+ + Br_2 \rightarrow MA + 2Br^- + 3H^+ + NH_2OH \quad (R12)$$

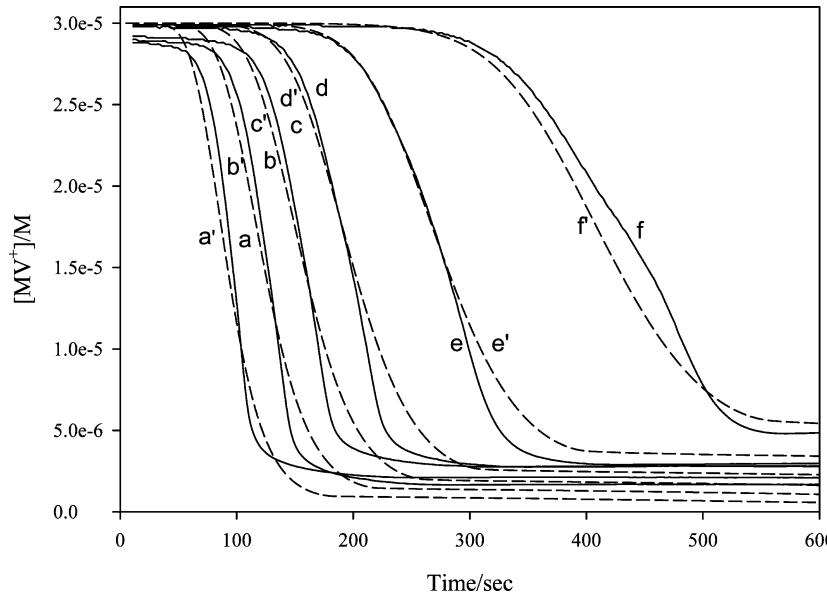

Figure 6. Kinetic profiles of initial bromate variation (experimental, solid lines (curves a−f); simulated, dashed lines (a′−f′)). (Conditions are the same as in Figure 2).

TABLE 5: Reaction Mechanism and Rate Coefficients Used for Simulations

reaction mechanism	rate coefficient
$2H^+ + BR^- + BRO_3^- \leftrightarrow HOBR + HBRO_2$	2.5, 3.2
$H^+ + BR^- + HBRO_2 \leftrightarrow 2HOBR$	2.5×10^6, 2×10^5
$H^+ + BR^- + HOBR \leftrightarrow BR_2$	8×10^9, 8
$HBRO_2 + H^+ \leftrightarrow H_2BRO_2^+$	2×10^6, 1×10^8
$HBRO_2 + H_2BRO_2^+ \rightarrow 2H^+ + HOBR + BRO_3^-$	1.7×10^5
$H^+ + BRO_3^- + HBRO_2 \leftrightarrow BR_2O_4$	4.8, 3.2×10^3
$BR_2O_4 \leftrightarrow 2BRO_2$*	7.5×10^4, 1.4×10^9
$MV^+ + BRO_3^- + H^+ \rightarrow MA + HBRO_2 + NH_2OH + H^+$	1.05×10^{-4}
$MV^+ + BRO_2$* $\rightarrow$ MVR+ + $HBRO_2$	2.44×10^5
$MVR^+ + BRO_2$* $\rightarrow MA + HBRO_2 + NH_2OH + H^+$	2.67×10^5
$MV^+ + HOBR \rightarrow MA + BR^- + 2H^+ + NH_2OH$	1.54×10^2
$MV^+ + BR_2 \rightarrow MA + 2BR^- + 3H^+ + NH_2OH$	1.15×10^2
$MV^+ + HBRO_2 \rightarrow MA + HOBR + NH_2OH + H^+$	6.51
$MA \rightarrow MP + HNEt_2$	2.3×10^6
$NH_2OH + HOBR \rightarrow HNO + BR^- + H^+$	2.27×10^3
$NH_2OH + BR_2 \rightarrow HNO + 2BR^- + 2H^+$	1.17×10^3
$HNEt_2 + BR_2 \rightarrow HONEt_2 + 2BR^- + 2H^+$	1.16×10^6
$HNEt_2 + HOBR \rightarrow HONEt_2 + BR^- + H^+$	2.06×10^3
$2HNO \rightarrow N_2O$	4.95×10^9

$$MV^+ + HBrO_2 \rightarrow MA + HOBr + NH_2OH + H^+ \quad (R13)$$

$$MA \rightarrow MP + HN(Et)_2 \quad (R14)$$

$$NH_2OH + HOBr \rightarrow HNO + Br^- + H^+ \quad (R15)$$

$$NH_2OH + Br_2 \rightarrow HNO + 2Br^- + 2H^+ \quad (R16)$$

$$HN(Et)_2 + Br_2 \rightarrow HON(Et)_2 + 2Br^- + 2H^+ \quad (R17)$$

$$HN(Et)_2 + HOBr \rightarrow HON(Et)_2 + Br^- + H^+ \quad (R18)$$

$$2HNO \rightarrow N_2O \quad (R19)$$

Both bromine and hypobromous acid are reactive intermediates that swiftly attack the methylene voilet and other organic intermediates. Relative levels of HOBr and Br_2 are dependent upon H^+ and Br^- ion concentrations (R3). The reaction of Br_2 with the organic moieties increases the concentration of bromide, which is an autocatalyst. The increase in [Br^-] exponentially increases Br_2 production ensuring rapid depletion of the reducing substrate. The bromination of aromatic substrates and formation of bromo or *N*-bromo transient intermediates in oxidation reactions involving bromine are well known.[11,22,23] The kinetics and reaction mechanisms get further complicated by the existence of a temporary sink for bromine which delays the generation of bromide. The brominated species upon further oxidation regenerate bromide. Taking into consideration the long induction time slight shift in the absorption peak with reaction progress (Figure 1a), a possible formation transient intermediates before the rapid depletion step, i.e., *N*-bromo species as the intermediates from the reactions of bromine or hypobromous acid with MV^+ cannot be completely ruled out. The relative importance of the bromination and oxidation rates by bromine and hypobromous acid differ with the nature of reducing substrates.

Simulations. To compute the characteristic features of the reaction, i.e. very slow initial phase followed by an instantaneous reaction, simulations were executed using the software "Simkine 2".[24,25] For the simulations, literature values were used for the rate constants of reactions R1−R7.[19,26] Experimental values from the current studies were employed for R8 and R14. A value taken from the literature was used for R19.[15] For the other steps,

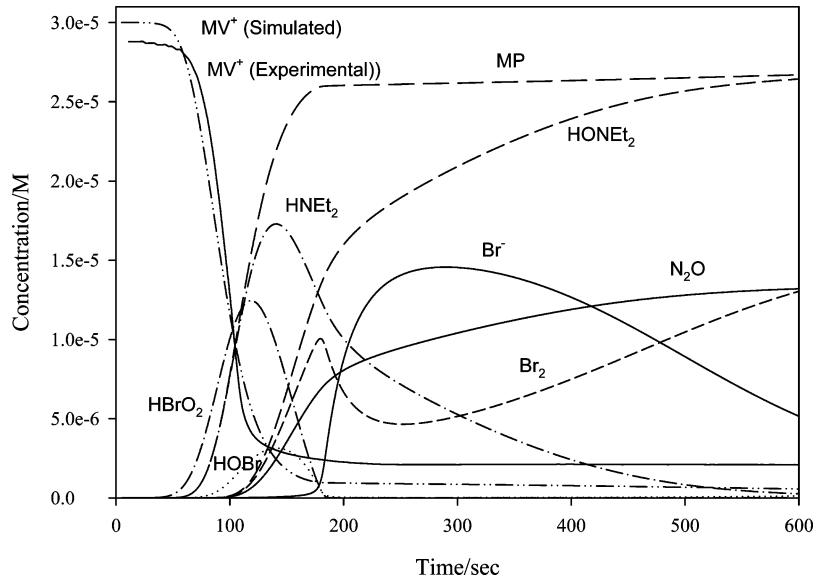

Figure 7. Simulated kinetic profiles of MV^+, intermediates, and products. $[MV^+]_0 = 3.0 \times 10^{-5}$ M, $[H^+]_0 = 0.2$ M, and $[BrO_3^-] = 0.02$ M.

SCHEME 1: Probable Intermediates during Oxidation

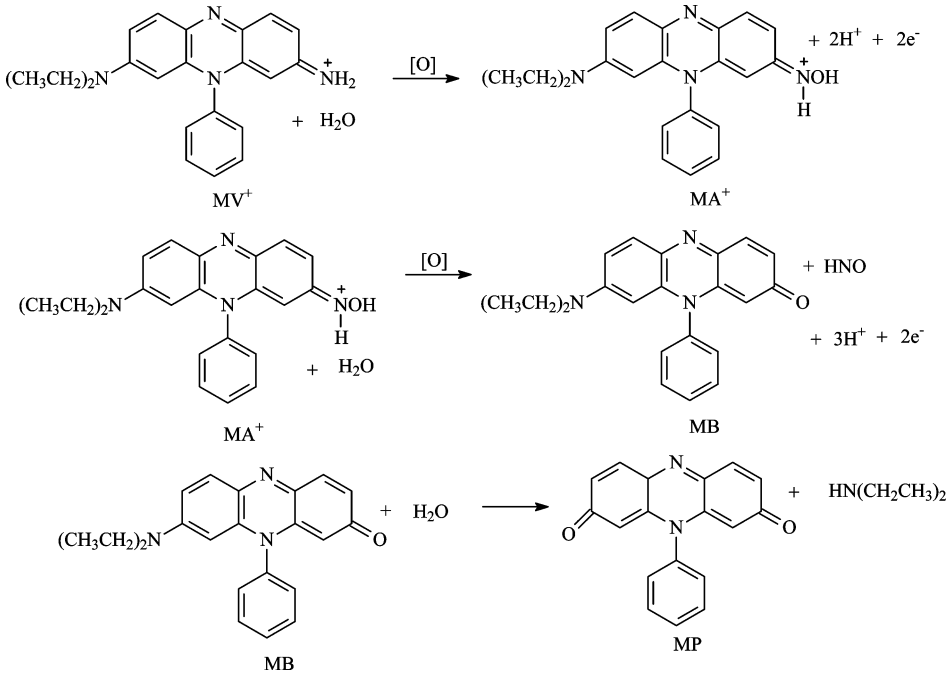

the estimated rate coefficients for reactions involving intermediates with bromo and oxybromo species were kept high, and values were adjusted such that the simulated curves agreed with the experimental curves. The rate coefficient for R8 was crucial as it is rate limiting. Table 5 summarizes all the elementary steps and rate coefficients used for the simulations. Figure 6 illustrates the experimental curves and corresponding simulated curves for the variation of initial bromate. A perusal of the profiles shows that the curves match fairly well with each other. Although the simulations could not entirely generate the sharp drop in MV^+ concentration, the simulated curves gave a good fit.

Figure 7 shows the experimental and simulated kinetic profiles of the $[MV^+]$. It also shows the simulated kinetic curves for various selected intermediates and products, including MP, which is the main oxidation product (see Scheme 1. In the simulated curves (Figure 7), the appearance of $HBrO_2$ and HOBr synchronized with the rapid depletion of MV^+, and the appearance of bromine and bromide sequence only after complete depletion MV^+ fully agree with proposed mechanism and the experimental profiles of bromine (Figure 4). Further, the simulated profiles of depletion of MV^+ in response to added bromide were also compiled (Figure 8). The satisfactory agreement between the experimental and simulated curves was observed. At low $[Br^-]_0$, simulations were sensitive to its change, and the experimentally observed prolonged induction times, with increase in added $[Br^-]$, could be reasonably simulated. In the simulations at high $[Br^-]_0$, although not exactly matched with an increase in bromide, the initial rates increased reflecting the trends of the experiment curves.

Parts a and b of Figure 9, respectively, illustrate the profiles of bromine and bromide with different added concentrations of initial bromide. Further, Figure 4 (curves a″, b″, d″, e″, and g″) and 9c (curves a‴, b‴, and d‴) show the profiles of the respective experimental curves for bromine and bromide levels.

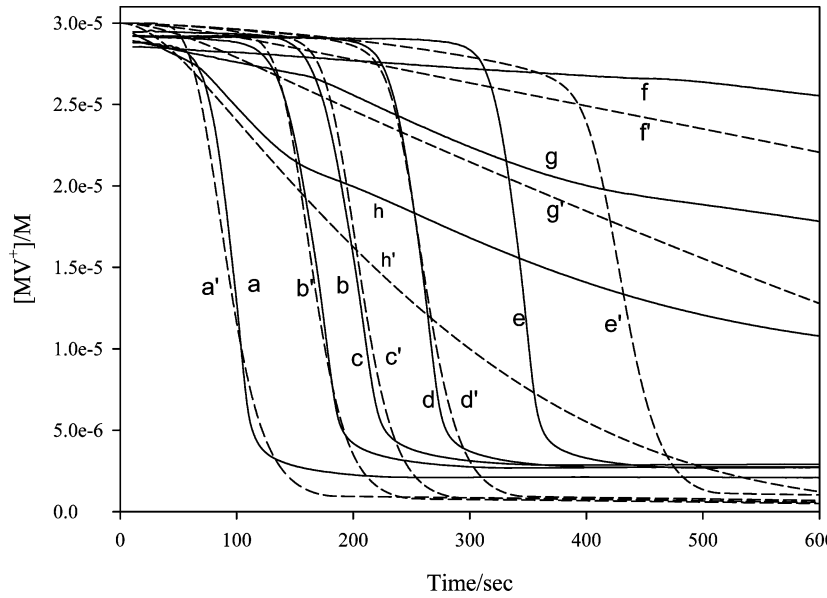

Figure 8. Kinetic profiles of MV^+ at varied $[Br^-]_0$ (experimental, solid lines (curves a−g); simulated, dashed lines (a′−g′)). (Conditions are the same as in Figure 4.)

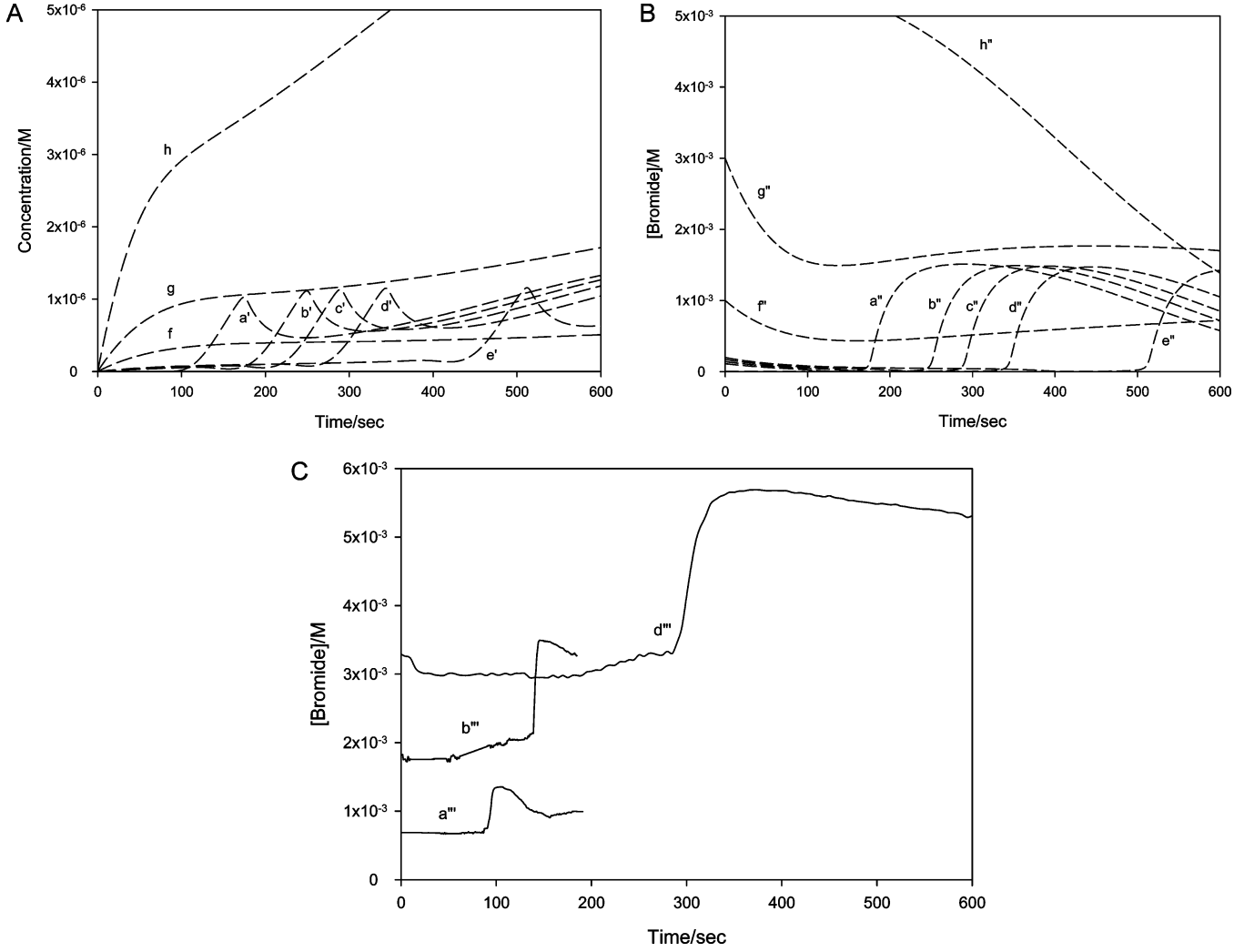

Figure 9. (a) Simulated kinetic profiles of Br_2 as function of added bromide. (Conditions are the same as in Figure 4.) (b) Simulated kinetic profiles of Br^- as function of added bromide. (Conditions same as in Figure 4.) (c) Experimental kinetic profiles of Br^- as function of added bromide. (Measured using a bromide ion selective electrode; conditions are the same as in Figure 4.) $[Br^-]_0$/M = curve a‴, Nil; b‴, 1.1×10^{-6}; d‴, 1.7×10^{-6}.

As the potentials were measured under stirred conditions, the induction times were slightly lower than the anticipated values [otherwise with spectrophotometric measurements. Unfortunately precise quantification of bromine and bromide concentra-

tions in the system is difficult. Although Br_2 has its absorption peak at 390 nm, in the presence of bromide it readily forms tribromide (Br_3^-), which has much higher absorption coefficient. Further, the measurement of absorbance at 270 nm corresponding to the tribromide maximum peak is not possible due to high absorption of organics present and dynamic bromine and bromide concentrations, which restrict the accurate determination of bromine in the system.[27,28] Similarly, the presence of other potentially interfering oxybromo species and chloride in the system, influence the reaction potential and limit the exact estimation of bromide concentration in the system.[29] The profiles of the experimental curves for bromine (Figure 4) and bromide (Figure 9c) agree satisfactorily with the simulated curves (parts a and b of Figure 9). There is good agreement between the profiles of the experimental and simulated curves, showing the effect of variation of initial [BrO_3^-] (Figure 6) and [Br^-] (Figure 8) on MV^+ depletion. Coupled with the profiles of Br^- and Br_2 with varying initial bromide concentration strongly supports and validates the proposed reaction scheme as the probable mechanism to explain the intricate reaction between MV^+ and acidic bromate. These simulations also support the assumption that, under low pH conditions, Br_2 is the crucial reactive intermediate to drive the rapid dynamics. The appearance of Br_2 in the simulation after the depletion of organic substrate further confirms that the bromine is the reactive intermediate and is maintained at steady state in equilibrium with HOBr.

Conclusions

This kinetic study elucidates the complex chemistry of MV^+/acidic bromate reaction. The simulated curves further support the experimentally predicted dominant role of bromine over hypobromous acid in the reaction. Further, the observed magnitude of the rates of depletion of MV^+ in the rapid stage with acidic bromate and, in the initial stages with high $[Br^-]_0$, also confirm the probable role of the bromide ion as an autocatalyst responsible for the rapid consumption of the dye after the induction time.

Acknowledgment. The authors thankfully acknowledge the financial support received from the University of KwaZulu-Natal and the National Research Foundation, Pretoria, South Africa. Authors also thank Ms. D. Moodley and Dr. M. K. Pillay for the help in characterization of the organic products.

References and Notes

(1) NIIR Board, The complete Technology Book on Dye and Dye intermediates, National Institute of Industrial Research, New Delhi, 2008.

(2) Satake, M.; Mido, T. *Chemistry of Colour*; Discovery Publishing House: New Delhi, 1995.

(3) Morley, J. S. *J. Chem. Soc.* **1952**, 4008.

(4) Zhang, X. Y.; Field, R. J. *J. Phys. Chem.* **1992**, *96*, 1224.

(5) Foersterling, H.; Varga, M. *J. Phys. Chem.* **1993**, *97*, 7932.

(6) Kurin-Csorgei, K.; Zhabotinsky, A. M.; Orban, M.; Epstein, I. R. *J. Phys. Chem.* **1996**, *100*, 1593.

(7) Simoyi, R. H.; Epstein, I. R.; Kustin, K. *J. Phys. Chem.* **1994**, *98*, 551.

(8) Muthakia, G. K.; Jonnalagadda, S. B. *J. Phys. Chem.* **1989**, *93*, 4751.

(9) Jonnalagadda, S. B.; Musengiwa, N. *Int. J. Chem. Kinet.* **1998**, *30*, 111.

(10) Jonnalagadda, S. B.; Salem, M. A. *PCCP* **1999**, *1*, 821.

(11) Jonnalagadda, S. B.; Gollapalli, N. R. *South Afr. J. Chem.* **2001**, *54*, 41.

(12) Grasselli, J. G.; Ritchey, W. M. *Atlas of Spectral Data and Physical Constants for Organic Compounds*, 2nd ed.; CRC Press, Cleveland, OH, 1975; *Vol. 1*.

(13) Paquette, L. A. *Principles of Modern Heterocyclic Chemistry*; W. A. Benzamin Inc., New York, 1968.

(14) Jonnalagadda, S. B.; Shezi, M.; Gollapalli, N. R. *Int. J. Chem. Kinet.* **2002**, *34*, 542.

(15) Granzow, A.; Abraham, W.; Fausto, R., Jr. *J. Am. Chem. Soc.* **1974**, *96*, 2454.

(16) Sullivan, J. C.; Thompson, R. C. *J. Inorg. Chem.* **1979**, *18*, 2375.

(17) Jonnalagadda, S. B. *Int. J. Chem. Kinet.* **1984**, *16*, 1287.

(18) Hasty, R. A.; Lima, E. J.; Ottaway, J. M. *Analyst* **1981**, *106*, 76.

(19) Jonnalagadda, S. B.; Simoyi, R. H.; Muthakia, G. K. *J. Chem. Soc., Perkin Trans 2* **1988**, 1111.

(20) Jocobs, S. S.; Epstein, I. R. *J. Am. Chem. Soc.* **1978**, *98* (7), 1721.

(21) Szalai, I.; Koros, E. *J. Phys. Chem.* **1998**, *102*, 6892.

(22) Elderfield, R. C. *Heterocyclic Compounds*, 2nd ed.; Chapman and Hall; New York, 1957; *Vol. 6*.

(23) Harrison, J. J.; Pellegrini, J. P.; Selwitz, C. M. *J. Org. Chem.* **1981**, *41*, 2169.

(24) Jonnalagadda, S. B.; Parmasur, N.; Shezi, M. N. *Comput. Biol. Chem.* **2003**, *27*, 147.

(25) Shezi, M. N.; Jonnalagadda, S. B. *South Afr. J. Chem.* **2006**, *59*, 82.

(26) Gyorgyi, L.; Varga, M.; Koros, E.; Field, R. J.; Ruoff, P. *J. Phys. Chem.* **1989**, *93*, 2836.

(27) Pink, J. M. *Can. J. Chem.* **1970**, *48*, 1169.

(28) Kerenskaya, G.; Goldschleger, I. U.; Apkarian, V. A.; Janda, K. C. *J. Phys. Chem. A* **2006**, *110*, 13792.

(29) Koryta, J. *Annu. Rev. Mater. Sci.* **1986**, *16*, 13.

JP810015P